

Supporting Text and Figures

Stochastic coordination of multiple actuators reduces latency and improves chemotactic response in bacteria

Michael W. Sneddon^{1,2}, William Pontius^{2,3} and Thierry Emonet^{1,2,3}

¹Interdepartmental Program in Computational Biology and Bioinformatics, Yale University, New Haven, CT

²Department of Molecular, Cellular and Developmental Biology, Yale University, New Haven, CT

³Department of Physics, Yale University, New Haven, CT

Contents

Extended description of the model of the flagellar motor	2
Extended description of the conformation model of multiple flagella	2
Analytical analysis of the conformation model of multiple flagella	3
Figure S1. Experimentally calibrated response of the single flagellar motor model	6
Figure S2. Effects of the characteristic waiting time spent in the semi-coiled form of the conformation model on run and tumble statistics	7
Figure S3. Steady-state statistics of for flagellar bundles which require $N-2$ flagella	8
Figure S4. Virtual experiments to measure response lag in terms of CW or tumble bias	9
Figure S5. Response lag for cells with high tumble biases	10
Figure S6. Assessing the magnitude and timescale of signaling noise in wild-type cells	11
Figure S7. Motor coordination as a function of the timescale of noise	12
Figure S8. Coordination of multiple flagella affects fluctuations of the tumble bias over time, but not the mean tumble bias as a function of [CheY-P]	13
Figure S9. Signaling noise and motor coordination extends run lengths and generates slow fluctuations in cell output.	14
Figure S10. Measuring the frequency response of the multiple flagella model	15
Figure S11. Effects of signaling noise on the frequency response of a cell.	16
Figure S12. Maximal duration of runs is limited by the timescale of signaling noise	17
Figure S13. Effective diffusion coefficient as a function of noise level for cells with the same mean concentration of CheY-P	18
Figure S14. Response of the chemotaxis model with multiple flagella to step increases of the chemoattractant methyl-aspartate	19
Figure S15. Advantage of noise on shallow gradients requires motor coordination	20
Supporting References	21

Extended description of the model of the flagellar motor.

Single motors were modeled as two-state systems where states correspond to clockwise (CW) or counter-clockwise (CCW) rotation (1-3). Transitions between states arise from thermal fluctuations that overcome the free energy barrier between states. The free energy barrier, ΔG , varies in time as a function of $Y_p = [\text{CheY-P}]$ and can be written as

$$\Delta G(t) = \frac{g_0}{4} - \frac{g_1}{2} \left(\frac{Y_p(t)}{Y_p(t) + K_D} \right), \quad (1)$$

where K_D is the binding constant of CheY-P to the base of the motor, and the free parameters g_0 and g_1 are in units of $k_B T$. It follows from a two-state model that the rate of switching between rotational states is

$$k_{\pm} = \omega \cdot e^{\pm \Delta G(t)}, \quad (2)$$

where k_+ is the rate of switching from CW to CCW states, k_- is the rate of switching from CCW to CW states, and ω is a scaling parameter that controls the timescale of switching events. Given k_+ and k_- , the CW bias of the motor, which is the probability that a motor is in CW rotation, is $k_- / (k_- + k_+)$. Additionally, the switching frequency of the motor is $k_- \cdot (1-B) + k_+ \cdot B$, where B is the CW bias (fraction of time spent in CW rotation). The parameters of the model were fixed as $K_D = 3.06 \mu\text{M}$, $g_0 = g_1 = 40 k_B T$ and $\omega = 1.3 \text{s}^{-1}$ to fit experimental data (4) as shown in Fig. S1.

Extended description of the conformation model of multiple flagella.

The conformation model of multiple flagella is a phenomenological model designed to capture the key conformational changes that each flagellum adopts during changes in the rotational state of the corresponding flagellar motor (5, 6). Therefore, in this model, the conformational state of each flagellum is explicitly tracked. Let $f_i(t)$ be the conformational state of flagellum i at time t , where $i=1 \dots N$ and N is the number of flagella. Let $m_i(t)$ be the rotational state, either CW or CCW, of motor i at time t . Finally, let $T_i^m(t)$ be the cumulative length of time that motor i has been in state $m_i(t)$. Then, the next conformational state of flagellum i after a small time step dt is determined according to the following update rules:

$$f_i(t+dt) = \begin{cases} \text{NORM} & \text{if } m_i(t+dt) = \text{CCW} \text{ and } T_i^m(t) > d + dt \\ \text{SEMI} & \text{if } m_i(t+dt) = \text{CW} \text{ and } d + dt < T_i^m(t) < d + \lambda_i + dt \\ \text{CURLY} & \text{if } m_i(t+dt) = \text{CW} \text{ and } T_i^m(t) > d + \lambda_i + dt \\ f_i(t) & \text{otherwise} \end{cases} \quad (3)$$

where λ_i is an exponentially distributed random number generated independently for flagellum i when that flagellum switches to semi-coiled and $d = 0.015 \text{s}$ is the time delay for a conformational change to propagate through the end of the flagellum (5).

Given $f_i(t)$, the run or tumble state of a cell at time t is determined as follows. If all flagella are in the normal conformation, then the cell is running. If any single flagellum is in the semi-coiled conformation, then the cell is tumbling. Finally, if there are a minimum number of flagella in the normal conformation to form a bundle, then flagella in the curly conformation can wrap around the bundle and the cell runs.

The conformation model has two free parameters: the mean waiting time before semi-coiled to curly transitions and the minimum number of motors in normal conformation needed to assemble a functional bundle. Unless otherwise specified, the mean waiting time of semi-coiled to curly transitions, $\bar{\lambda}$, was set to 0.2s and the minimum number of flagella needed to form a bundle, x , was set to 2.

Analytical analysis of the conformation model of multiple flagella.

An analytic description of the conformation model requires an expression for the tumble bias of the cell and the rate of switching between run and tumble states in terms of the CheY-P concentration and the parameters of the model. First, we calculate the probability that a cell is running, $P(c=RUN)$, which is the tumble bias of the cell. For a cell, c , with N flagella to be in the *RUN* state there must be at least x flagella in the normal conformation and no flagella in the semi-coiled conformation, where x is the threshold number of flagella needed to form a coherent bundle. Ignoring the short time delay, d , between motor switching and a change in flagella conformation, there are three possible states that a motor/flagellum pair can exist as: 1) CW and semi-coiled; 2) CW and curly; and 3) CCW and normal. For motor/flagellum pair i , we can calculate the joint probability that a motor and flagellum are in particular states as:

$$\begin{aligned}
 \text{State 1: } P(m_i=CW, f_i=SEMI) &= P_1 = P(f_i=SEMI | m_i=CW) \cdot P(m_i=CW) \\
 \text{State 2: } P(m_i=CW, f_i=CURLY) &= P_2 = (1 - P(f_i=SEMI | m_i=CW)) \cdot P(m_i=CW) \\
 \text{State 3: } P(m_i=CCW, f_i=NORM) &= P_3 = 1 - P(m_i=CW)
 \end{aligned}$$

We note that $P(m_i=CW) = k_-/(k_-+k_+)$, which is the CW Bias of the motor where k_- and k_+ , defined in equation 2, are the rates of switching from the *CCW* to *CW* and *CW* to *CCW* respectively, as defined in the main text. Furthermore, $P(f_i=SEMI | m_i=CW)$ depends on k_+ , the rate that the motor switches to *CCW* rotation, and $\bar{\lambda}$, the mean rate that the flagellum switches from semi-coiled to curly and can be written as:

$$P(f_i=SEMI | m_i=CW) = k_+ / (\bar{\lambda}^{-1} + k_+) \quad (4)$$

To be in the *RUN* state, there must be zero motor/flagellum pairs in State 1 and greater than or equal to x motor/flagellum pairs in State 3. Thus, we calculate $P(c=RUN)$ by summing over the multinomial distribution for all cases where the number of flagella in State 3 is greater or equal to x and no flagellum is in State 1, which is:

$$P(c=RUN) = \sum_{j=x}^N \frac{N!}{0!(N-j)!j!} \cdot P_1^0 \cdot P_2^{N-j} \cdot P_3^j \quad (5)$$

Note that in this notation, P_1 is equivalent to the probability P_{SEMI} , P_2 is equivalent to the probability P_{CURLY} and P_3 is equivalent to P_{NORMAL} , which were the probabilities given in the main text. This expression can also be rewritten directly in terms of the flagellar motor and conformation model parameters as:

$$P(c=RUN) = \sum_{j=x}^N \frac{N!}{(N-j)!j!} \cdot \left(\frac{k_- \cdot \bar{\lambda}^{-1}}{(k_- + k_+) \cdot (k_+ + \bar{\lambda}^{-1})} \right)^{N-j} \cdot \left(\frac{k_+}{k_- + k_+} \right)^j \quad (6)$$

As $k_- + k_+$ are functions of $[\text{CheY-P}]$, we immediately have the tumble bias of a cell as a function of $[\text{CheY-P}]$. Note that $P(c=TUMBLE) = 1 - P(c=RUN)$.

Next, we calculate the tumble rate for a cell again assuming that the delay d between motor switching and a change in flagella conformation is negligible. A cell will enter the *TUMBLE* state whenever a single motor in *CCW* switches to *CW* rotation. Motors switch independently, so given j motors in *CCW*, the rate that any one motor switches to *CW* and thus induces a tumble is $j \cdot k_-$. Then, the overall rate, k_T , that a cell will switch to a *TUMBLE* is the sum over all possible j cases weighted by the probability that a cell in the *RUN* state has j motors in *CCW*. This calculation is equivalent to multiplying k_- by the average number of flagella in the normal conformation given that the cell is running, as described in the main text. So we have

$$k_T = \sum_{j=x}^N j \cdot k_- \cdot P(n_{CCW} = j | c = RUN) \quad (7)$$

where n_{CCW} is the number of motors in *CCW*. To calculate the conditional probability, $P(n_{CCW} = j | c = RUN)$, we rewrite the probability as

$$P(n_{CCW} = j | c = RUN) = [P(c = RUN | n_{CCW} = j) \cdot P(n_{CCW} = j)] / P(c = RUN) \quad (8)$$

We already have $P(c = RUN)$ from the above calculations. Additionally, we can calculate $P(n_{CCW} = j)$ using the binomial distribution as

$$P(n_{CCW} = j) = \binom{N}{j} \cdot (1 - P(m_i = CW))^j \cdot P(m_i = CW)^{N-j} \quad (9)$$

Then, we can compute the conditional probability $P(c = RUN | n_{CCW} = j)$, by simply noting that the probability for a cell to be in the *RUN* state with j motors in *CCW* is equivalent to the

probability that given $N - j$ motors in CW, none are in the semi-coiled conformation. From above, we have $P(f_i=SEMI | m_i=CW) = k_+ / (\bar{\lambda}^{-1} + k_+)$, thus

$$P(c = RUN | n_{CCW} = j) = [1 - (k_+ / (\bar{\lambda}^{-1} + k_+))]^{N-j} \quad (10)$$

Finally, we can calculate both the rate with which a cell switches from the *TUMBLE* state to the *RUN* state, k_R , and the overall switching frequency, SF , between *TUMBLE* and *RUN* states by solving for k_R in terms of the tumble rate and the tumble bias of the cell, which gives:

$$k_R = k_T \cdot (1 - P(c=TUMBLE)) / P(c=TUMBLE) \quad (11)$$

$$SF = k_T \cdot (1 - P(c=TUMBLE)) + k_R \cdot P(c=TUMBLE) \quad (12)$$

Figure S1. Experimentally calibrated response of the single flagellar motor model. The model of a single flagellar motor (black lines) was calibrated to fit the motor response measured experimentally (4) (open circles) in terms of (A) the probability to be in CW rotation (CW Bias) and (B) the frequency of switching between rotational states. Parameters used for this fit are $K_D = 3.06\mu\text{M}$, $g_0 = g_1 = 40k_B T$ and $\omega = 1.3\text{s}^{-1}$.

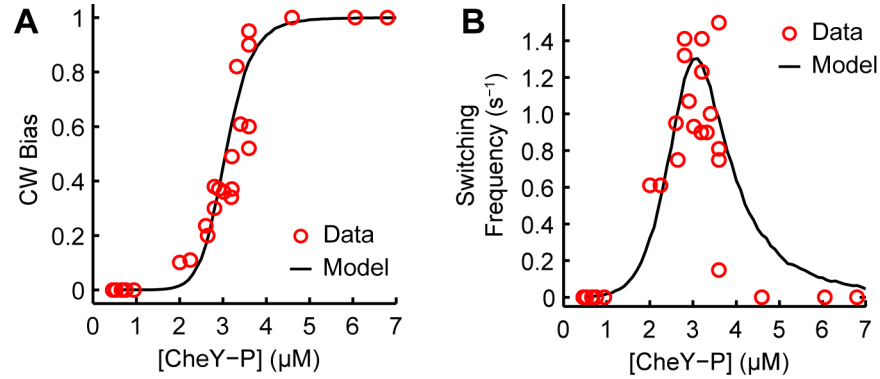


Figure S2. Effects of the characteristic waiting time spent in the semi-coiled form of the conformation model on run and tumble statistics. (A) Tumble bias of the cell as a function of the characteristic semi-coiled waiting time parameter for cells with 3 flagella (blue solid line), 4 flagella (red dashed line) and 5 flagella (green dashed-dotted line). (B) Mean run duration as a function of the waiting time parameter for the same cells. (C) Mean tumble duration as a function of the waiting time parameter for the same cells. All cells in these simulations have flagellar motors with a CW bias of 0.15 and signaling noise with a CV = 0.1 and time correlation = 30s. For simulations reported in the main text, we selected the characteristic waiting time so that a typical cell with 3-4 flagella will have a tumble bias that is similar to the CW bias of its individual motors and a mean run duration of approximately 0.8s.

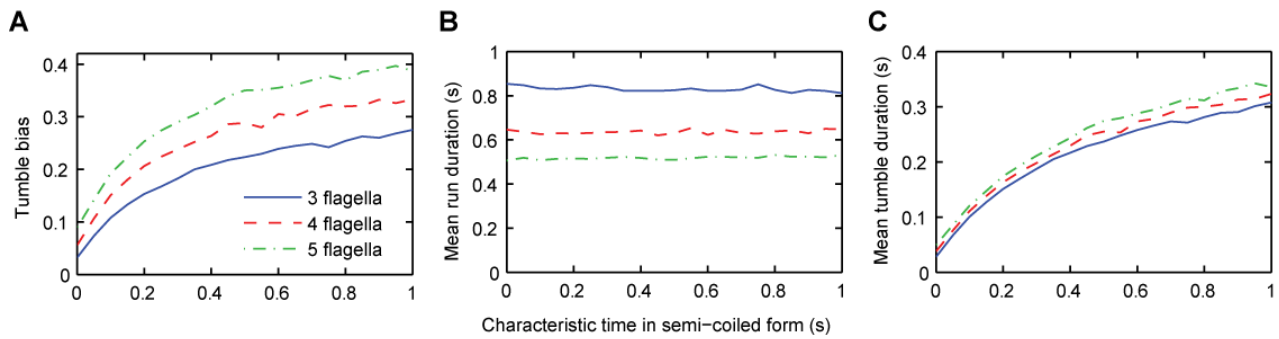


Figure S3. In our model, for a cell with N flagella to be running, no flagella can be in semi-coiled and a minimum number of flagella, x , must be in the normal conformation to form a bundle. In the main text we analyzed the cases in which cells have either a single flagellum or 3, 4 or 6 flagella with $x = 2$. Here we explore the consequences of requiring that all flagella but two be in the normal confirmation for the bundle to exist, $x = N - 2$. As in Fig. 2 of the main text, we examine the run and tumble statistics for unstimulated cells. Note that curves for 4 flagella are identical to those in the main text. (A) The probability to be tumbling (tumble bias) and (B) the rate of switching between run and tumble states based on the conformation model where x is set to $N - 2$ for cells with either 3 (red), 4 (black) or 6 (blue) flagella. For the case of 6 flagella, $x = 4$ requires more flagella to form a coherent bundle as compared to the main text: the tumble bias curve is accordingly shifted to the left. For $N = 3$, only one flagellum is required for bundle formation and the tumble bias curve is shifted to the right. The switching frequency curves are shifted so that their maxima correspond with a tumble bias of 0.5, but their magnitudes are not significantly affected. (C) The rate that a cell with 3 (red), 4 (black) or 6 (blue) flagella switches to a tumble as a function of tumble bias for $x = N - 2$. (D) The rate that a cell with 3 (red), 4 (black) or 6 (blue) flagella switches to a run as a function of tumble bias for $x = N - 2$. Like the overall switching rate, these rates are not very sensitive to changes in the minimum number of flagella to form a bundle.

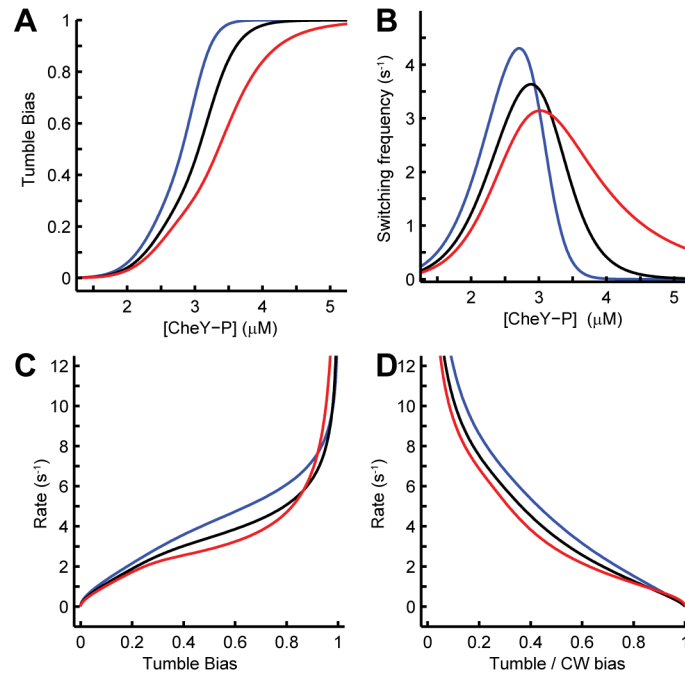


Figure S4. Virtual experiments to measure response lag in terms of the CW bias of a single motor of tethered cells or the tumble bias of freely swimming cells. (A) We performed a virtual experiment of 500 tethered cells and 500 swimming cells subject to a step decrease in CheY-P of $0.4\mu\text{M}$ at time zero to compare to the measurements in (7). The original experiments measured the response of tethered (single motor) or free swimming cells (multiple motors) to step increases in the chemoattractant L-aspartate by recording the CW bias of single motors or the frame-to-frame change in angular trajectory of swimming cells (proportional to the tumble bias) respectively. We performed a similar virtual experiment with our model by plotting the average CW bias of single motors or the tumble bias of swimming cells at 0.005s time resolution. Our simulations are consistent with the original experimental result which showed no appreciable difference between the response times of tethered and free swimming cells. This result demonstrates that although our model predicts a difference in response latency of $\sim 0.09\text{s}$, measurements of average CW or tumble bias of populations of up to 500 cells are not sensitive enough to reliably detect the $\sim 0.09\text{s}$ difference. (B) In contrast, our simulations do predict that comparisons using this metric to step increases in CheY-P (from either addition of repellent (8), or removal of attractant, shown here for a $0.4\mu\text{M}$ increase in $[\text{CheY-P}]$) should be detectable by experiments because the predicted reduction in latency is much greater ($\sim 0.5\text{s}$) between tethered and free swimming cells. For consistency with SI Ref (7), cells in both (A) and (B) have a mean CW or tumble bias of 0.35 .

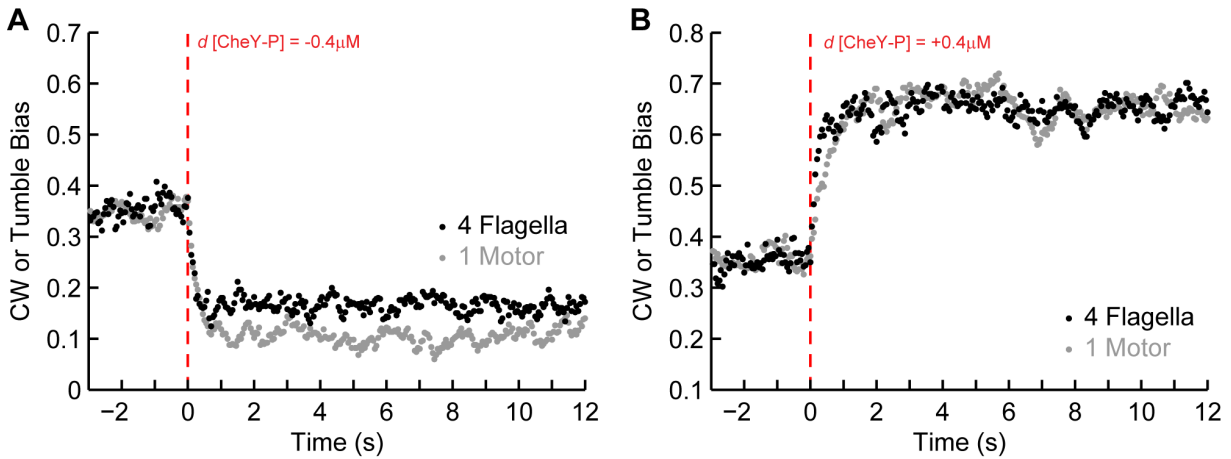


Figure S5. Response lag for cells with high tumble biases. (A) Response lag to step increases in [CheY-P] for cells with one (gray) or four (black) flagellar motors, computed as the mean time to switch from a run to a tumble after presentation of the stimulus as shown in the inset. (B) Response lag to step decreases in [CheY-P] for cells with one (gray) or four (black) flagellar motors computed as the mean time to switch from a tumble to a run after presentation of the stimulus. In (A) and (B), the initial value of [CheY-P] was chosen so that each cell has a tumble or CW bias of 0.78 ($3.4 \mu\text{M}$ for a cell with one flagellum and $3.48 \mu\text{M}$ for a cell with four flagella). Open circles are results of numerical simulations and lines are to guide the eye.

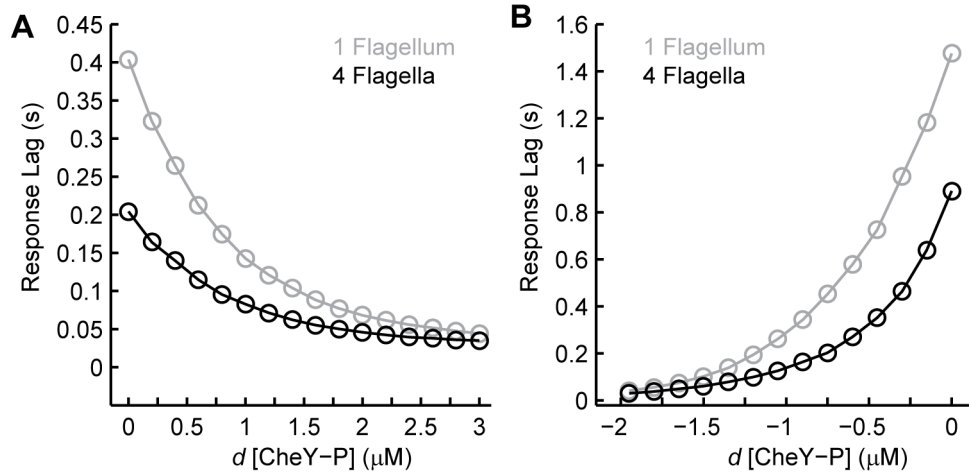


Figure S6. Assessing the magnitude and timescale of signaling noise in wild-type cells. (A) The power spectrum of motor output for a single, representative, non-stimulated, wild-type cell demonstrating noise at low frequencies (black) as compared to the power spectrum from a PS2001 mutant cell expressing CheYD13K, a constitutively active form of CheY (gray) (9). (B) The power spectrum of a simulated flagellar motor with input signaling noise in CheY-P with 30s time correlation and a CV of 0.15 (black), and without noisy input (gray).

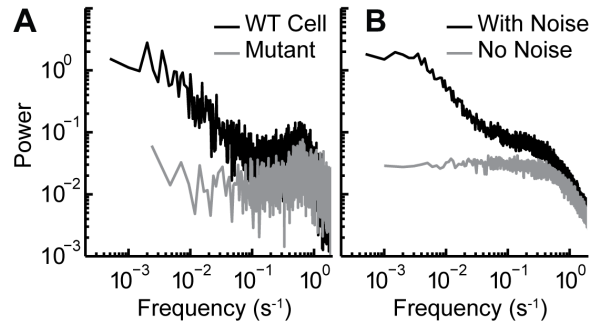


Figure S7. Motor coordination as a function of the timescale of noise. (A) Coordination of motors is computed as the linear (Pearson) correlation coefficient and is plotted as a function of the timescale of the signaling noise for different magnitudes of signaling noise, as indicated. (B) Same data as in (A), but plotted on a linear axis. In both (A) and (B), the dashed line indicates the approximate timescale of motor switching (1s). Note that these figures depict the same data that is plotted in Fig. 4B of the main text.

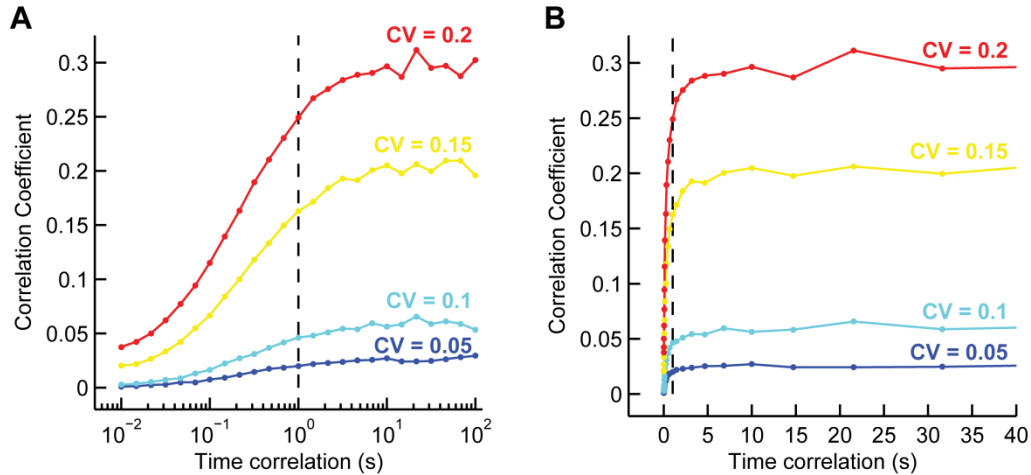


Figure S8. Coordination of multiple flagella affects fluctuations of the tumble bias over time, but not the mean tumble bias as a function of [CheY-P]. (A) Representative tumble bias over time of a cell with four flagella when motors are coordinated (black) compared to when motors are not coordinated (gray) even though the input [CheY-P] trajectories have the same magnitude and timescale of input noise ($CV = 0.15$, time correlation = 30s (9)). The bias trace is computed by taking the sliding average of the probability of the cell to be in the tumble state with overlapping 15s windows. Although not shown for clarity, cells with no input noise have similar profiles as a cell with uncoordinated motors. (B) The tumble bias for a cell with coordinated motors (black) and uncoordinated motors (gray), both with signaling noise similar to that measured in wild-type cells ($CV = 0.15$, time correlation = 30s), as a function of [CheY-P]. The CW bias of a single flagellar motor (dashed black line) demonstrates that the CheY-P response curve of the cell is similar to the response of a single motor.

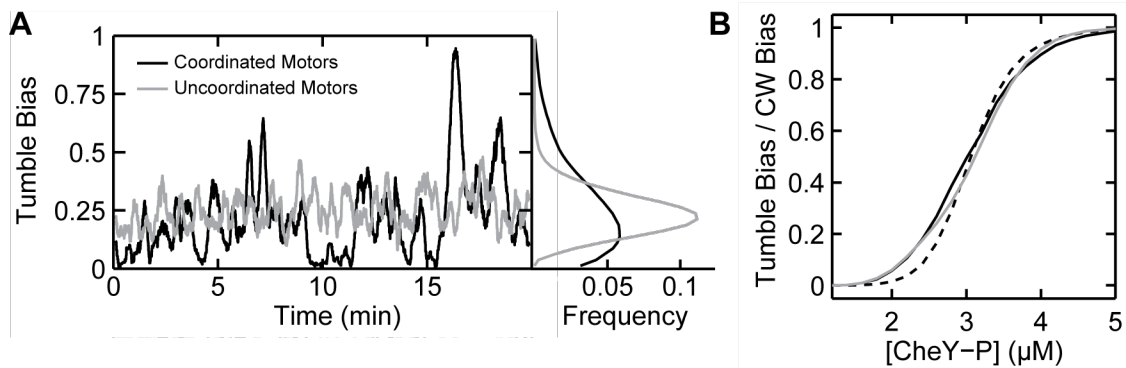


Figure S9. Signaling noise and motor coordination extends run lengths and generates slow fluctuations in cell output. (A) The distribution of run lengths and (B) the corresponding power spectra of the run/tumble trajectory of a cell with coordinated (black) and uncoordinated (gray) motors, both with noise with a CV of 0.15, time correlation of 30s, and output tumble biases of 0.25 (9). Coordinated motors receive the exact same input [CheY-P] trajectory, while uncoordinated motors receive two different input trajectories both with the same magnitude and timescale of fluctuations.

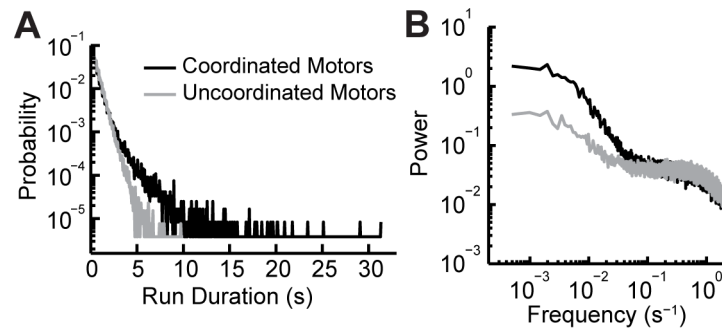


Figure S10. Measuring the frequency response of the multiple flagella model. To measure the signal-to-noise ratio of the multiple flagella model as reported in the main text, low amplitude, sinusoidal signals in [CheY-P] were passed as input, and the cellular response, measured as the binary trace of runs and tumbles was recorded. The power spectrum of the cellular response was computed (black), as shown in the example power spectrum depicted here. The peak in the power spectrum at the signal frequency was automatically detected (blue points). A flanking region of the power spectrum (red points) was also automatically identified and fit to a straight line (green). To calculate the signal-to-noise ratio, the integrated power at the signal frequency (area below the blue points and above the green line) was normalized by the total noise intensity (total area below the black curve, but not above the green line). Inset shows a close-up of the power spectrum around the signal frequency.

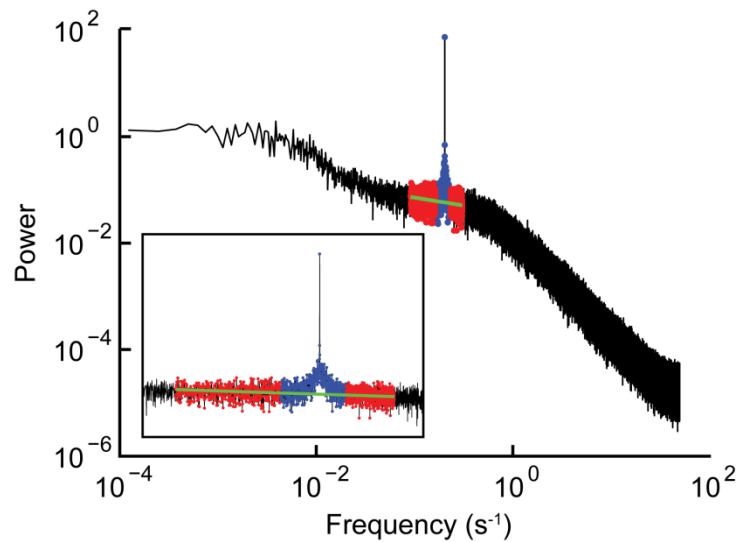


Figure S11. Effects of signaling noise on the frequency response of a cell. The frequency response to periodic stimuli in [CheY-P] with amplitude of $1\mu\text{M}$ for a cell with four flagella for cases with no noise in the input (solid gray line), noise with a CV of 0.15 and time correlation of 15s, and noise at high frequencies with a CV of 0.15 and a time correlation of 1s (dashed gray line). SNR for each point was computed over 20 replicates of 60,000s simulations. Error bars show the standard deviation of the measure over the 20 replicates. While the SNR decreased overall for both low and high frequency noise, the low frequency noise did not significantly degrade signals at timescales $\sim 10\text{s}$, indicating that the system with slow fluctuations operates as a band-pass filter governed by the timescale of fluctuations and the timescale of motor switching. On the other hand, if high frequency noise is considered, signals were uniformly degraded across all input frequencies.

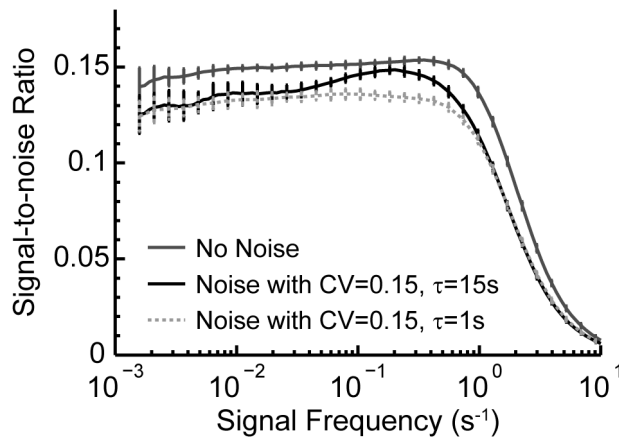


Figure S12. Maximal duration of runs is limited by the timescale of signaling noise. (A) Cumulative probability distribution of run lengths of cells with four flagella having threshold motors, i.e. a motor that always rotates CCW when [CheY-P] is below a threshold and rotates CW otherwise, with noise at 1s, 15s, 30s or 45s timescales (τ). A threshold motor ensures that any fluctuation, regardless of strength, about the threshold is fully amplified and immediately induces CW or CCW rotation of the motor. Thus, a threshold motor represents the theoretical maximum amount that the run length distribution of a cell could be extended due to noise. As shown, this limit depends on the timescale of the fluctuations. The threshold is set such that the tumble bias (TB) for all cells is 0.25. (B) Cumulative probability distributions for cells with four flagella with varying magnitudes of noise (dashed lines) as compared to the theoretical limit based on a cell with threshold motors (solid line). The timescale of the fluctuations is set to 30s, and the mean [CheY-P] is set such that each cell has a tumble bias of 0.25 regardless of the noise strength. Therefore differences in the run length distribution are related to noise intensity only, and not to changes in the tumble bias. (C) Same as (B), except that [CheY-P] was fixed at $2.55\mu\text{M}$, which implies that cells with higher noise strengths will have a higher tumble bias. All results were compiled from 100,000s long simulations of a single cell.

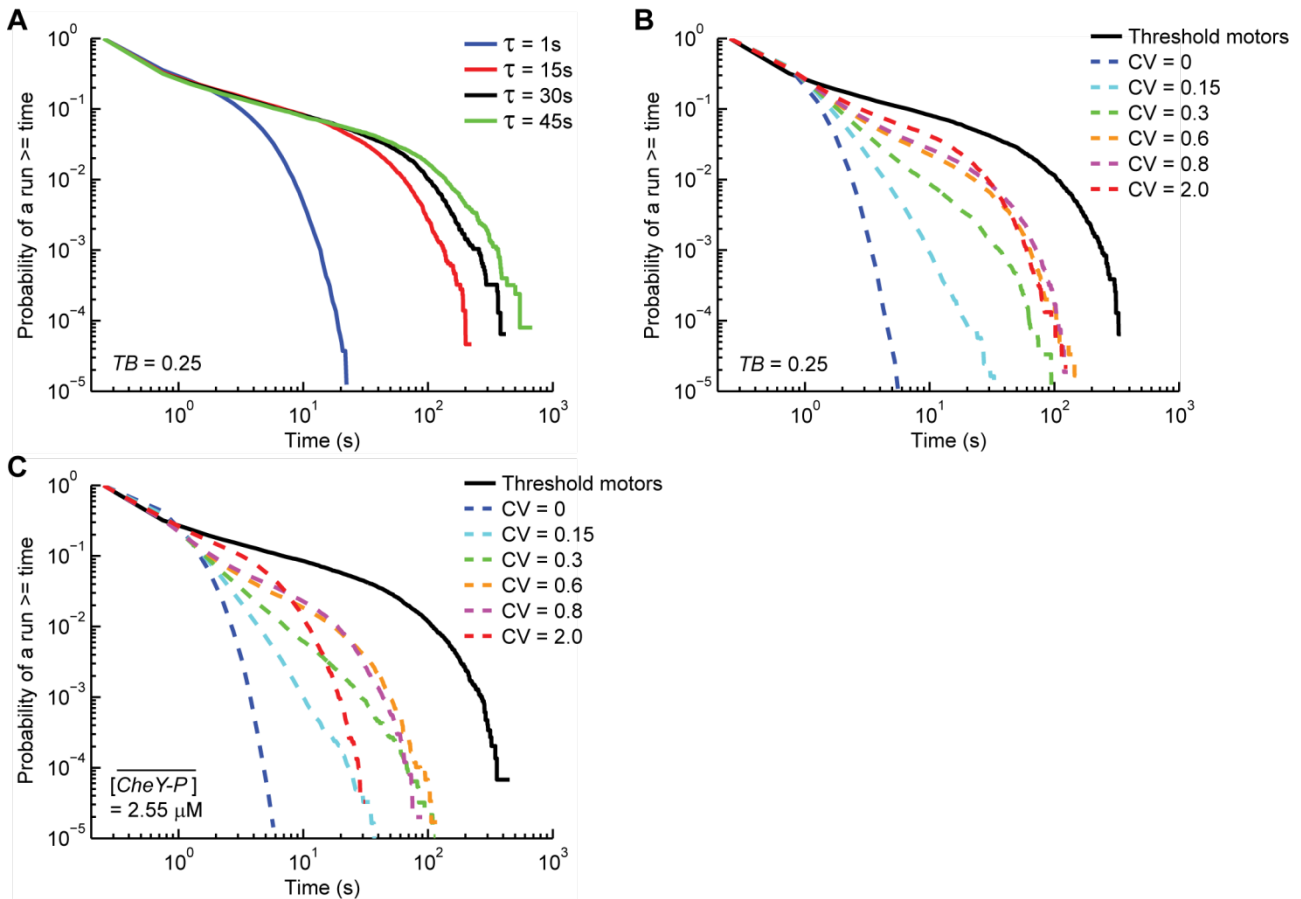


Figure S13. Effective diffusion coefficient as a function of noise level for cells with the same mean concentration of CheY-P. (A) Results are shown for populations of cells with coordinated (black) and uncoordinated motors (gray) and with either three (squares), four (circles), or six (triangles) motors per cell. (B) Effective diffusion coefficient for cells with four flagella and coordinated motors with a rotational diffusion constant of either $0.031 \text{ rad}^2/\text{s}$ (red), $0.062 \text{ rad}^2/\text{s}$ (black) and $0.124 \text{ rad}^2/\text{s}$ (blue). Similar to the results presented in Figure 4 of the main text, the effective diffusion coefficient saturates at levels of noise with a CV of approximately 0.6. All cells have a mean [CheY-P] of $2.55 \mu\text{M}$ and an adaptation time of 15s. Results were averaged over 4000 cells for each population.

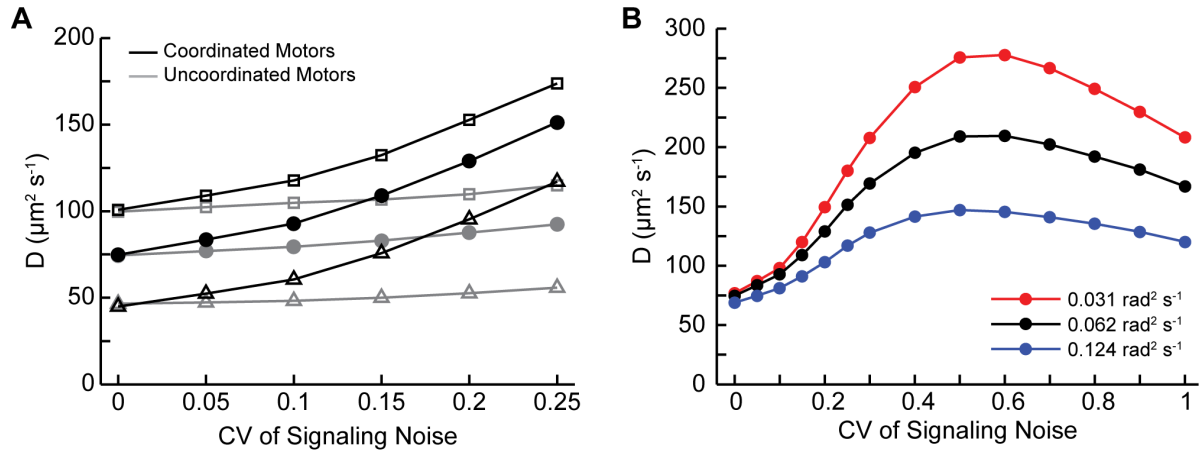


Figure S14. Response of the chemotaxis model with multiple flagella to step increases of the chemoattractant methyl-aspartate. (A) Response of the signaling system to increasing steps (0.001mM, 0.01 mM, 0.1 mM, 1 mM, 10 mM, and 100 mM) of methyl-aspartate measured as a concentration of CheY-P either with low noise (CV of 0.01, blue) or for the cell wild-type from Ref. (9) with noise with a CV of 0.15 and a time correlation of 30s. (B) Response of the system with four flagella measured as the tumble bias over time for a single cell with either coordinated motors (black) or uncoordinated motors (gray). Both cells have signaling noise with a CV of 0.15 and a time correlation of 30s. The tumble bias was computed as a 15s sliding average of the run and tumble trajectory of the cell.

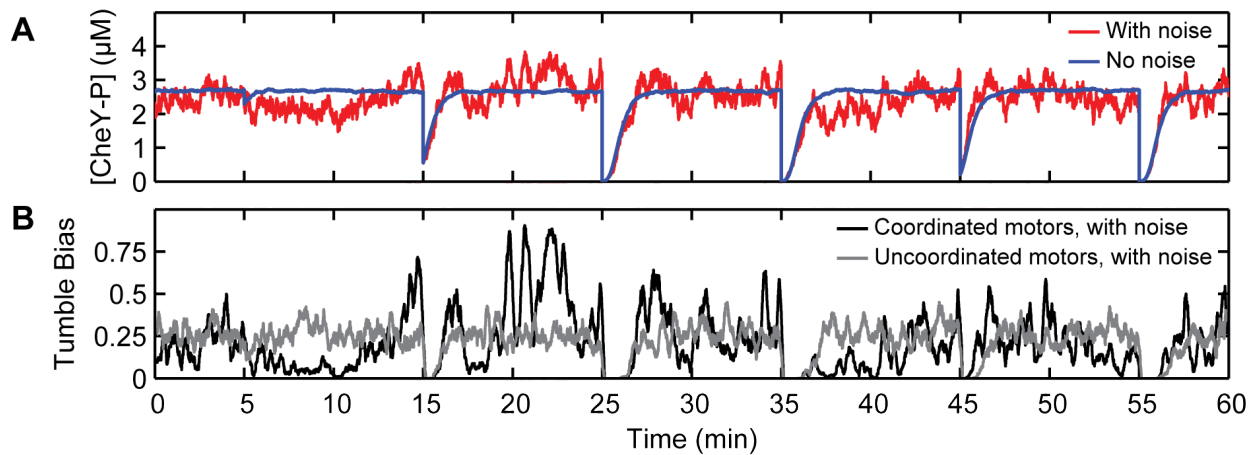
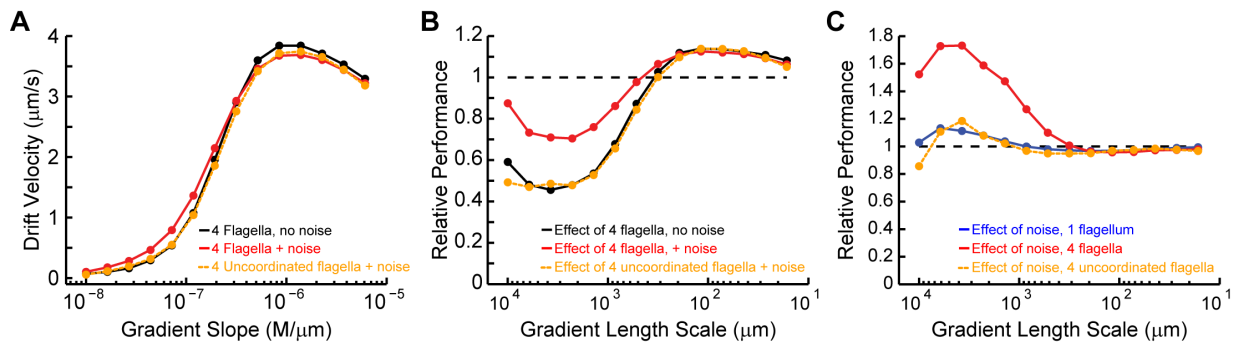


Figure S15. Advantage of noise on shallow gradients requires motor coordination. (A) Instantaneous drift velocity as a function of slope on linear gradients of methyl-aspartate measured at one minute after the start of the simulation for cells with four flagella and either no noise (black), noise of CV 0.15 (red), or noise of CV 0.15 with artificially uncoordinated motors (orange). Uncoordinated cells have equally noisy, but independent CheY-P signals for each of the four motors. Cells begin adapted to the initial background concentration of 0.1mM. Results were averaged over 18,000 cells for each population. All cells have a tumble bias of 0.25 and an adaptation timescale of 15s. (B) Relative effect of multiple motors on chemotactic performance shown for the case of uncoordinated motors. Note that the advantage of noise on shallow gradients is eliminated for cells with uncoordinated motors. (C) Relative effect of signaling noise on chemotactic performance, which again demonstrates that coordination of motors is required to maximize the beneficial effect of noise. As in the main text, the length scale of the linear gradient is calculated as $L/(dL/dx)$ at the initial position of the cell where the ligand concentration is $L=0.1\text{mM}$. We note that the results for cells with a single flagellum and coordinated flagella reported here are the same data as in Fig. 3 of the main text.



Supporting References

1. Fall C, Marland E, Wagner J, & Tyson J (2005) *Computational Cell Biology* (Springer).
2. Tu Y & Grinstein G (2005) How White Noise Generates Power-Law Switching in Bacterial Flagellar Motors. *Phys Rev Lett.* 94(20):208101-208101.
3. Sneddon MW, Faeder JR, & Emonet T (2011) Efficient modeling, simulation and coarse-graining of biological complexity with NFsim. *Nat Methods* 8(2):177-183.
4. Cluzel P, Surette M, & Leibler S (2000) An Ultrasensitive Bacterial Motor Revealed by Monitoring Signaling Proteins in Single Cells. *Science* 287(5458):1652-1655.
5. Darnton NC, Turner L, Rojevsky S, & Berg HC (2007) On Torque and Tumbling in Swimming *Escherichia coli*. *J Bacteriol.* 189(5):1756-1764.
6. Turner L, Ryu WS, & Berg HC (2000) Real-time imaging of fluorescent flagellar filaments. *J Bacteriol.* 182(10):2793-2801.
7. Jasuja R, Keyoung J, Reid GP, Trentham DR, & Khan S (1999) Chemotactic responses of *Escherichia coli* to small jumps of photoreleased L-aspartate. *Biophys J.* 76(3):1706-1719.
8. Khan S, Jain S, Reid GP, & Trentham DR (2004) The fast tumble signal in bacterial chemotaxis. *Biophys J.* 86(6):4049-4058.
9. Korobkova E, Emonet T, Vilar JMG, Shimizu TS, & Cluzel P (2004) From molecular noise to behavioural variability in a single bacterium. *Nature* 428(6982):574-578.